

Stochastic Resonance in Bistable and Excitable Systems

Sean Rhett-Burke Bearden
UCSD, Physics Department
(Dated: November 29, 2016)

In detection theory, stochastic resonance refers to a class of randomness-enhanced phenomena concerning signal processing. Stochastic resonance was first proposed to explain the periodic ice ages of Earth. While originally defined in a narrow context, the usefulness of stochastic resonance to describe behavior observed in physical systems has led to an expansion of the definition. This report will consider the two systems extensively studied in the literature: bistable and excitable systems. Manifestations of stochastic resonance are observed in numerical simulations of these systems using *Wolfram Mathematica 11*.

I. INTRODUCTION

The term *stochastic resonance* appeared in a 1981 paper concerning the periodic behavior of the Earth's ice ages [1]. (The term had been used prior to 1981 to refer to an unrelated phenomenon [2].) The term, as it is used today, is meant "...to describe any phenomenon where the presence of internal noise or external input noise in a nonlinear system provides a better system response to a certain input signal than in the absence of noise" [2]. The occurrence of stochastic resonance in a system is easily understood from the curve in Fig. 1. The requirement that the system be nonlinear comes from the fact that in a linear system (linear referring to the output signal being a linear transform of the input signal) the output signal has an optimal signal-to-noise ratio (SNR) when no noise is present.

While SNR can be used to quantify stochastic resonance, it is not always an appropriate measure. Other forms of measurement of output performance include spectral power amplification, correlation coefficient, mutual information, and Kullback entropy.

Stochastic resonance falls under a class of randomness-enhanced phenomena, with many examples in literature prior to the 1981 paper from Benzi, *et al.* [1]. For stochastic resonance, the phenomenon that is enhanced by randomness is a signal, and only occurs in this context. That is, stochastic resonance achieves maximal performance in the output signal when there is a presence of noise.

II. HISTORICAL OVERVIEW

The field of stochastic resonance began to grow shortly after the publication of Ref. [1] in 1981. However, it has been shown that Peter Debye's 1929 publication on the dielectric properties of polar molecules in a solid [4] can be reinterpreted to encompass stochastic resonance [5]. This is the earliest known analytical result for the susceptibility of a fluctuating symmetrical system with two coexisting stable states [2].

Early on, stochastic resonance was a term only used in the context of a bistable system driven by a combina-

tion of a periodic force and random noise. Observation in experiment came from two different bistable systems: In 1983 stochastic resonance was observed in a Schmitt trigger electronic circuit [6], and in 1988 stochastic resonance was observed in a bidirectional ring laser [7]. Both systems are bistable systems, leading some to believe that bistability was a necessary condition for stochastic resonance to occur. Using linear response theory, it was shown that stochastic resonance can occur without bistability [5]. Experimental observation of stochastic resonance in a monostable system occurred in 1993 [8].

From 1993 to 1996, the field of stochastic resonance expanded considerably. No longer constrained to the context of a bistable system, stochastic resonance was applied to investigation of neural systems and excitable systems. After 1996, the main developments led to the discovery of aperiodic stochastic resonance, where aperiodic input signals can showcase stochastic resonance. Modern applications of stochastic resonance are too extensive to detail in this report. The reader is directed to Ch. 2 of Ref. [2] for a descriptive outline of applications.

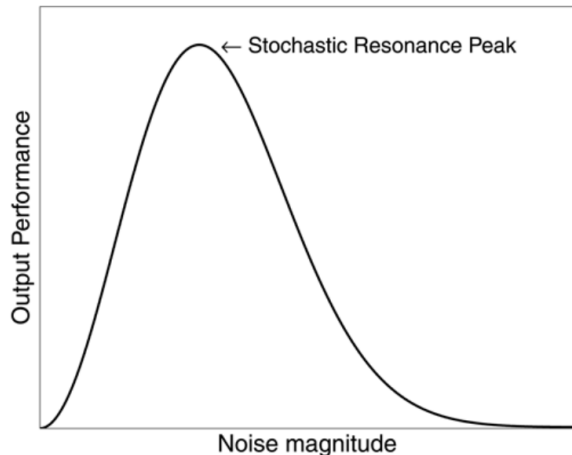


FIG. 1. A qualitative plot of output performance vs. noise magnitude. Contrary to intuition, a peak in performance is observed when noise is nonzero. (Image taken from Ref. [3].)

III. BISTABLE SYSTEMS

A bistable system with a reflection-symmetric, quartic potential energy can be modeled as:

$$U(x) = -\frac{a}{2}x^2 + \frac{b}{4}x^4, \quad (1)$$

with $a, b > 0$. A simplification of this continuous potential is a discrete two-state system. Let us begin by developing a description of the discrete case, then develop the continuous case.

In the presence of a periodic driving signal, stochastic resonance will occur when the period of the signal is matched to some characteristic time of the system. Kramers' rate, r_K , can be used to characterize the system in the absence of the driving signal. (That is, the characteristic escape rate from a well of the potential in the absence of a driving signal.) The inverse of Kramers' rate gives the average time between hopping events. Intuitively, the period of the driving signal should be twice the inverse of Kramer's rate to optimize the probability of noise-induced hopping events. The intuition: the driving signal modifies ("tilts") the minima of the potential, with each of the two minima being raised (at different times) during one period of the driving signal. This is the time-scale matching condition for stochastic resonance [9].

A. Discrete Two-State System

Consider a general case of a two-state system with known transition rates: $W_{\pm}(t)$. The transition rates are a function of input noise and possibly other parameters. For the following description to hold, the adiabatic limit must hold. That is, the frequency of the driving signal is much lower than the inverse of some relaxation time in the system. In this double-well system, the relaxation time is given by the time it takes for probability to equilibrate within one well [10].

The dynamics can be described with the master equation (in integer state space):

$$\dot{n}_{\pm} = -W_{\mp}(t)n_{\pm} + W_{\pm}(t)n_{\mp}, \quad (2)$$

where $n_{\pm}(t)$ is the probability the system occupies the \pm state at time t . The solution to Eq. 2 is given in Ref. [9] as:

$$n_{\pm}(t) = g(t) \left[n_{\pm}(t_0) + \int_{t_0}^t W_{\pm}(\tau)g^{-1}(\tau)d\tau \right], \quad (3)$$

$$g(t) = \exp \left[- \int_{t_0}^t W_{+}(\tau) + W_{-}(\tau)d\tau \right],$$

where $n_{\pm}(t_0)$ is an initial condition. To proceed any further, the transitions rates of interest must be known.

B. Continuous Bistable Potential

If the system of interest has a continuous bistable potential, e.g., Eq. 1, a Fokker-Planck description of the dynamics can be applied. Let us start with the Langevin equation modeling a Brownian particle of mass m moving in a bistable potential $U(x)$, exposed to thermal noise $\xi(t)$ of the Nyquist type at temperature T , with a periodic perturbation term in the rate equation:

$$m\ddot{x} = -m\gamma\dot{x} - U'(x) + mA\cos(\Omega t + \phi) + \sqrt{2m\gamma kT}\xi(t), \quad (4)$$

where x represents the state of the system, γ is the friction coefficient, and k is the Boltzmann constant [9]. For the external forcing term, A is the amplitude, Ω is the angular frequency, and ϕ is the initial phase. The noise term, $\xi(t)$, has properties:

$$\langle \xi(t) \rangle = 0, \quad \langle \xi(t)\xi(t+\tau) \rangle = \delta(\tau). \quad (5)$$

A two-dimensional Fokker-Planck equation can be derived from Eq. 4:

$$\frac{\partial}{\partial t}p(x, v, t; \phi) = \left\{ -\frac{\partial}{\partial x}v + \frac{\partial}{\partial v} \left[\gamma v - \frac{U'(x)}{m} - A\cos(\Omega t + \phi) \right] + \gamma D \frac{\partial^2}{\partial v^2} \right\} p(x, v, t; \phi), \quad (6)$$

where $v = \dot{x}$ and $D = \frac{kT}{m}$.

In the case of large friction, Eq. 4 is reduced by applying adiabatic elimination on the velocity variable, v . While the general, rigorous application of adiabatic elimination is too extensive to outline here (see Ref. [11]), it suffices to consider Eq. 4 when $|\gamma\dot{x}| \gg |\ddot{x}|$. This consideration results in an overdamped Langevin equation:

$$\gamma\dot{x} = -\frac{U'(x)}{m} + A\cos(\Omega t + \phi) + \sqrt{2\gamma D}\xi(t) \quad (7)$$

The mass variable, m , is absorbed into a and b of Eq. 1, then variables are rescaled:

$$\bar{x} = x/x_m, \quad \bar{t} = at/\gamma, \quad \bar{A} = A/ax_m \quad (8)$$

$$\bar{D} = D/ax_m^2, \quad \bar{\Omega} = \gamma\Omega/a.$$

where $x_m = \sqrt{a/b}$ is the distance of both minima of $U(x)$ from the origin. The resulting dimensionless Fokker-Planck equation is given by:

$$\frac{\partial}{\partial \bar{t}}p(\bar{x}, \bar{t}; \phi) = [\mathcal{L}_0 + \mathcal{L}_{ext}(\bar{t})]p(\bar{x}, \bar{t}; \phi), \quad (9)$$

$$\mathcal{L}_0 = -\frac{\partial}{\partial \bar{x}}(\bar{x} - \bar{x}^3) + \bar{D}\frac{\partial^2}{\partial \bar{x}^2},$$

$$\mathcal{L}_{ext}(\bar{t}) = -\bar{A}\cos(\bar{\Omega}\bar{t} + \phi)\frac{\partial}{\partial \bar{x}},$$

which is the Smoluchowski limit of Eq. 6. This is to be expected due to applying adiabatic elimination, as the Smoluchowski limit procedure is the prototype to all adiabatic elimination [12].

C. Kramers' Rate

If the driving signal is absent in Eq. 7, then there will still be a small probability for a transition to occur. Kramers' method [13] is used to derive the average time, T_K , for the system to transition from one potential well to the other. The inverse of T_K is Kramers' rate:

$$r_K = \frac{\sqrt{U''(a)|U''(0)|}}{2\pi} \exp(-\Delta U/D). \quad (10)$$

where ΔU is the barrier height.

As a consequence of ignoring the driving signal, the derived value of D below will be independent of amplitude, A , when applying the time-scale matching condition. Clearly, stochastic resonance will depend on A , so Kramers' rate only gives an approximation to the dynamic rate of hopping events.

D. Example

Let us look at a simple example of stochastic resonance in an overdamped bistable potential given by scaling Eq. 7 to be dimensionless:

$$\dot{x} = x - x^3 + A \cos(\Omega t) + \sqrt{2D}\xi(t) \quad (11)$$

where the bars above the variables has been dropped, $\phi = 0$, and $\sqrt{\gamma/a}$ has been absorbed into $\xi(t)$. The rescaled noise, $\xi(t)$, will have the same properties given in Eq. 5. The rescaled potential is given by Eq. 1 with $a = b = 1$, where minima occur at $x_m = \pm 1$. There is also a local maximum at $x = 0$. The difference in $U(x)$ at the minimum and maximum defines the barrier height, which is found to be $\Delta U = \frac{1}{4}$.

The dynamics of the system are investigated by considering various values of the noise intensity, D , in Fig. 2. In the absence of noise, the driving signal is not strong enough to cause the system to transition from one minimum to the other. Likewise, the noise is not strong enough (in a probabilistic sense) to cause a transition. However, when both the driving signal and the noise are present, there exists a nonzero probability of the system making a transition.

At the beginning of this section, it was pointed out that stochastic resonance occurs when the time-scale matching condition ($2T_K = T_\Omega$) is achieved. Using Eq. 10:

$$2\sqrt{2\pi}e^{\Delta U/D} = \frac{2\pi}{\Omega}, \quad (12)$$

from which the optimal noise magnitude is derived as:

$$D = \frac{-\Delta U}{\ln(\sqrt{2}\Omega)}. \quad (13)$$

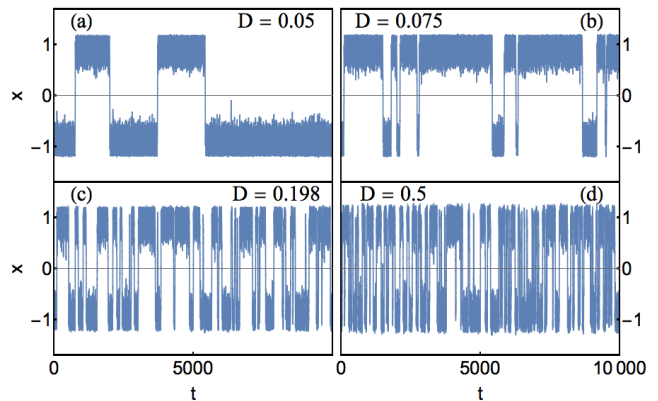


FIG. 2. Solutions to Eq. 11 with $x(0) = -1$, $A = 0.43$, $\Omega = 0.2$, with increasing noise amplitude, D . Transitions are identified when the signal crosses $x = 0$

It is required that $\Omega < \frac{1}{\sqrt{2}}$ so that D is positive.

The following analysis is qualitative due to necessarily long computations times required to evaluate output signal quality. For purposes of comparison, the noise term $\xi(t)$ is the same random variable in each plot of Fig. 2. Only the noise magnitude D is different. For simulations, the values used are $x(0) = -1$, $A = 0.43$, and $\Omega = 0.2$.

First, let us examine a solution to Eq. 11 where D is small. In Fig. 2(a), the system exhibits a transition, though it does not appear to be periodic. (Transitions are identified when the signal crosses $x = 0$.) However, there are clearly time intervals of stability, so D should be close to the choice of noise magnitude that optimizes stochastic resonance. In Fig. 2(c), the predicted optimal noise magnitude determined from Eq. 13 is used. There are many transitions, where periodicity is not immediately apparent, but there are time intervals of stability. In Fig. 2(d), the noise magnitude is too large, and, as a consequence, the hopping events are seemingly-chaotic. Turning our attention to Fig. 2(b), there appears to be approximately 3 periods of a periodic signal. Of course, further computation would need to be performed to confirm the periodicity of this signal.

To give an interpretation of the model, let us examine Benzi's research on the Earth's ice ages [1, 14, 15]. In that description, the bistable potential represents the Earth's climate, with each of the two minima representing the glacial and interglacial periods. The driving signal is interpreted to be small planetary gravitational perturbations in the orbital eccentricity of Earth, occurring on a time scale of approximately 10^5 years. The noise can be attributed to annual fluctuation in solar radiations. In fact, variation in solar energy influx is approximately 0.1%, so modeling the fluctuations as a seemingly-small amount of noise is appropriate. The theory proposes that the variation in solar energy influx is of appropriate magnitude to cause stochastic resonance, which results in periodic ice ages.

IV. EXCITABLE SYSTEMS

Initially, only bistable systems had been the subject of stochastic resonance research. Historically, excitable systems were the next focus of research [9]. An excitable system has only one stable state, but can transition into a nonstable excited state when some threshold within the system is overcome. The excited state will decay on a time scale that is long compared to the relaxation rate of small perturbations about the stable state.

Longtin applied stochastic resonance in excitable systems to neuron models in 1993 [16]. The development of stochastic resonance in excitable and threshold dynamical systems spawned the application of stochastic resonance in neurophysiology [9].

To understand stochastic resonance in excitable systems, consider two types of signals: subthreshold and suprathreshold. In a subthreshold system, the input signal does not cross some threshold for signal detection to be possible. By adding noise to a system, signals that would have been undetectable can now cross the threshold of detection. In a suprathreshold system, the input signal partially crosses the threshold of detection, though the detection may not accurately represent the entire signal.

Stochastic resonance can occur in the case of a periodic input signal or an aperiodic input signal, but the method of recovering the signal is different in either case. Periodic signals will be considered in this section. The treatment of aperiodic signals can be shown, but SNR will have no meaning in this context. Instead, Shannon mutual information is used as the measure of stochastic resonance [17].

A. Subthreshold System Example

In a subthreshold system with periodic input signal, stochastic resonance can occur when noise is added to the system so that the signal may now cross the threshold of the detector. To reconstruct the signal, it is sampled at some specified rate and signal interpretation rules outlined in Refs. [18, 19] are used. If the sample point is above the threshold, but the previous sample point was below threshold, then it is registered as a crossing (quantified simply as 1). This is a threshold crossing with positive slope. No other sequence of sample points registers as a crossing in this algorithm (quantified as 0). A periodogram is used to approximate the spectral power density of the resulting sequence of zeros and ones. If stochastic resonance has occurred, it will manifest in the frequency components of the input signal in the spectral power density.

To give an example, a periodic input signal $x(t)$ is distorted with additive white Gaussian noise. The choice of periodic signal is given by:

$$x(t) = \sin(0.5t) + \sin(2t). \quad (14)$$

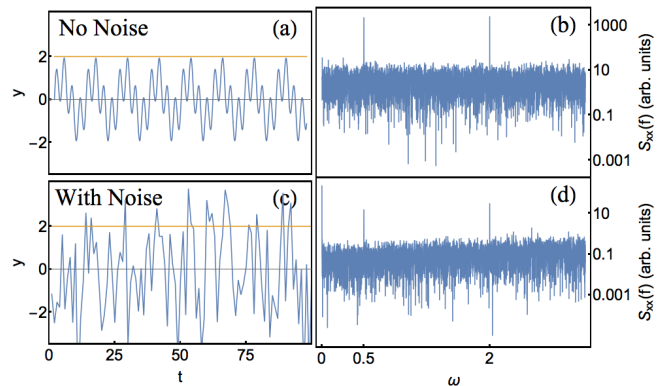


FIG. 3. A periodic signal (a) without noise and (c) with noise. The yellow line in (a) and (c) represents the detection threshold. In (b) the signal (ignoring the detection threshold) is sampled 10^4 times at integer values of t to produce the estimated power spectrum. The two frequency components of the signal manifest as peaks. In (d) the power spectrum is estimated from the signal with noise (applying the detection threshold) sampled 10^4 times at integer values of t then converted into binary (as described elsewhere).

In the absence of noise, the output signal $y(t)$ is equal to the input signal. The output signal with no noise is shown in Fig. 3(a). The yellow line represents the threshold above which the output signal can be detected. The output signal never crosses the threshold value, so it cannot be detected. In Fig. 3(b), the detection threshold is ignored, so the power spectrum of the input signal can be used for comparison. Clearly, the two frequency components of Eq. 14 are observed: $\omega_1 = 0.5s^{-1}$ and $\omega_2 = 2s^{-1}$.

In Fig. 3(c), the input signal is subjected to zero-mean internal noise $\xi(t)$ with autocorrelation given by $\langle \xi(t)\xi(t+\tau) \rangle = 4\delta(\tau)$. The signal as shown is constructed by sampling the signal with noise at integer values of t . Threshold crossings are more probable to occur when the input signal is close to the threshold value, and less probable to occur when the input signal is near its minimum.

The output signal used in Fig. 3(d) was sampled 10^4 times, where the detection threshold is used. Clearly, the two signal frequencies are recovered, but at a loss of 2 magnitudes of power.

B. Optimal Stochastic Resonance in Subthreshold Systems

To computationally test for optimal stochastic resonance in a subthreshold system, an input signal, $x(t) = \sin(1.25t)$, is used with a simulated detector with a threshold equal the signal's amplitude ($x = 1$). Zero-mean noise with autocorrelation given as $\langle \xi(t)\xi(t+\tau) \rangle = 2D\delta(\tau)$ is added to the signal. As D is varied, the height of the $\omega = 1.25s^{-1}$ peak above the spectral background is measured. In this example, the profile of the noise $\xi(t)$

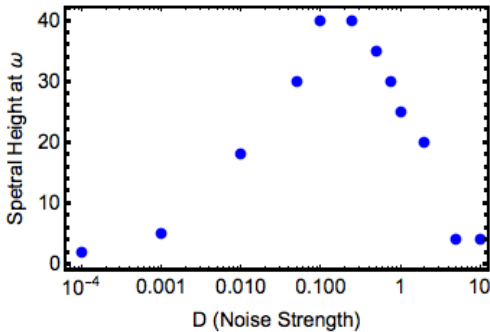


FIG. 4. Stochastic Resonance in a subthreshold system for varying noise amplitude, D . Compare with the qualitative curve in Fig. 1

is randomized for each value of D tested. This is done to show that the exact profile of the noise is not important

when testing for stochastic resonance.

The signal detection process described in the previous subsection was followed for 12 different values of D . In Fig. 4, the approximate spectral peak height (arbitrary units) is plotted as a function of D . The observed output performance curve is similar to that in Fig. 1.

V. ACKNOWLEDGEMENTS

Much of the Historical Overview section is a synopsis of chapter 2 of Ref. [2]. For a more detailed discussion of topics herein, the reader is directed to the review paper cited in Ref. [9], which has served as a guide in writing the section on bistable systems, and Ref. [18], which is the source of most of the excitable systems section. All calculations were performed with *Wolfram Mathematica 11*.

-
- [1] R. Benzi, A. Sutera, and A. Vulpiani, *Journal of Physics A: Mathematical and General*, **14**, L453-L457 (1981).
 - [2] M. D. McDonnell, N. G. Stocks, C. E. M. Pearce, and D. Abbott, *Stochastic Resonance: From Suprathreshold Stochastic Resonance to Stochastic Signal Quantization* (Cambridge University Press, New York, 2008).
 - [3] M. D. McDonnell and D. Abbott, *PLoS Computational Biology*, **5**(5): e1000348.
 - [4] P. J. W. Debye, *Chemical Catalog Company, Incorporated*, Polar Molecules (1929).
 - [5] M. I. Dykman, *et al.*, *Il Nuovo Cimento D*, **17**, 661-683 (1995).
 - [6] S. Fauve and F. Heslot, *Physics Letters A*, **97**(1), 5-7 (1983).
 - [7] B. McNamara, *et al.*, *Physical Review Letters*, **60**, 2626 (1988).
 - [8] N. G. Stocks, *et al.*, *Journal of Physics A: Mathematical and General*, **26**, L385-L390 (1993).
 - [9] L. Gammaitoni, *et al.*, *Reviews of Modern Physics*, **70**(1), (1998).
 - [10] B. McNamara and K. Wiesenfeld, *Phys. Rev. A*, **39**(9), (1989).
 - [11] H. Risken, *The Fokker-Planck Equation: Methods of Solutions and Applications* (Springer, USA, 2009), p.188.
 - [12] C. Gardiner, *Stochastic Methods: A Handbook for the Natural and Social Sciences, 2nd Ed.* (Springer, New York, 1989), p.192-193.
 - [13] Ref. [12], pp. 378-382.
 - [14] R. Benzi, *et al.*, *em Tellus*, **34**(1), 10-16 (1982).
 - [15] R. Benzi, *et al.*, *SIAM J. on Applied Math.*, **43**(3), 565-578 (1983).
 - [16] A. Longtin, *J. Stat. Phys.*, **70**, 309, (1993).
 - [17] A. R. Bulsara and A. Zador, *Phys. Rev. E*, **54**(3), (1996).
 - [18] K. Wiesenfeld and F. Moss. *Phys. Rev. Lett.* **72**(14), (1994).
 - [19] K. Wiesenfeld and F. Moss. *Nature* **373**.6509, 33-36 (1995).